ORIGINAL PAPER

Á. Szűcs · M. Novák

Simultaneous electrochemical and piezoelectric microgravimetry measurements of C_{60} films with a quartz crystal microbalance in a dimethylformamide-water mixed solvent solution containing potassium ions

Abstract Simultaneous electrochemistry and piezoelectric microgravimetry studies using electrochemical quartz crystal microbalance were carried out on solution cast C_{60} films. These films could be reduced in dimethylformamide + water mixture containing potassium ions. It was established that the first reduction was a completely surface-confined process, while the second reduction produced dissolved species. Restricting the potential range only to the first reduction, we could observe reversible electrochemical transformation of the films. Measuring the mass changes of the electrodes during the electrochemical processes, we found that the "simple" voltammograms (single reduction and oxidation peaks) actually cover simultaneous processes. Both the reduction and the oxidation involved the movements of anions, cations and solvent molecules in and out of the films. It was measured that the initial behavior of the films varied "randomly", probably depending on the unpredictable structure of the film produced by solution casting. However, the films adjusted themselves to the experimental conditions displaying "steady-state" behavior after a certain number of potential scans. This "steady-state" behavior could be reached independently of the original structure, or the amount of C_{60} put on the surface, but it could be perturbed easily by altering the conditions. The films were self-adjusted to the measurements.

Á. Szűcs (✉) · M. Novák
Department of Physical Chemistry,
University of Szeged,
6701 Szeged, P.O. BOX 105,
Hungary
E-mail: aszucs@chem.u-szeged.hu
Tel.: +36-62-544627
Fax: +36-62-544652

Introduction

Electrochemical investigation of fullerenes in solid state started long ago [1–6]. Most of the early studies were carried out in acetonitrile containing various electrolytes. In those solutions reversible electrochemical reduction of C_{60} could be observed with suitable, large cations, such as tetraalkylammonium cations, when the potential range was restricted to the first and second one-electron reduction. The reduction mechanism was also investigated by quartz crystal microbalance studies [2, 4, 7–10], and it was established that significant structural change of the fullerene films occurred during the electrochemical processes. The reduction involved the uptake of the cations of the electrolytes to compensate the negative charge on the fullerene. However, in some studies, it was shown that the oxidation did not release these cations, instead an anion movement in the film was suggested. Investigations were carried out with films of various structure. Solution cast [8–11], physically adsorbed [12–15], and electrochemically deposited [2, 7] films were studied, as well. Some characteristic differences between these were suggested; however, sometimes similar films were observed to behave differently. In acetonitrile solutions, fullerene films reacted irreversibly in the presence of small metal cations such as alkali [1, 7, 9, 16]. Both irreversible intercalation, and dissolution of the reduced C_{60} was suggested. Recently, we discovered that in dimethylformamide + water mixtures of proper composition C_{60} could be reduced reversibly if the solution contained potassium ions [17]. By electrochemical measurements, we suggested a reduction mechanism, which involved structural rearrangement of the film to accommodate the counter ions, and upon oxidation we suggested the possibility of anion uptake simultaneously to cation release. We expanded

those investigations, and with the use of a quartz crystal microbalance, we could follow the mass changes during the electrochemical processes, and thus, we could refine the suggestions on the mechanism. These new results and hypotheses are summarized in this study.

Materials and methods

Materials

The electrode was a gold disc of 5.1 mm in diameter deposited on a quartz plate of 13.7 mm in diameter. The quartz was an AT cut, polished, mounted, and bonded 10 MHz crystal from International Crystal Manufacturing Co., OK, USA. The mass sensitivity of the crystal was calculated to be 0.86 ng Hz^{-1} [18]. C_{60} (MER, 99.99% purity) was deposited onto the disc from 300 μM dichloromethane (Sigma, HPLC grade) solution. The solution for the measurements was 1 M KCl (Reanal, analytical grade) in 48 v/v% dimethylformamide (Merck, spectroscopic grade) + water (Millipore, Milli-Q) mixtures. The solutions were deaerated with high purity nitrogen gas saturated by dimethylformamide vapor.

Electrode preparation

The electrode surfaces were washed with dichloromethane and dried under a heat gun. Then the C_{60} solution was put on them in 3–5 μl portions with prewarming of the electrode surface before each portion. As the drop of C_{60} solution was drying, the electrode was rotated slowly to provide more uniform covering of the surface. Finally, the electrode was rinsed with Millipore water and dried. Microscopic pictures of a film formed from a 50 μl solution can be seen in Fig. 1. Figure 1a shows that the film was not uniform. Toward the center of the gold disc, the film was thicker (darker), and some stripes can be seen due to the flow of the drop, as we rotated the electrode. At higher magnification (Fig. 1b), however, it is clear, that only a few larger crystals (black spots) were produced with this technique, and the gold remained uncovered (white spots) only around these crystals. So, we may say that the films were not even, but rather coherent, and slightly crystalline. In Fig. 1c, it can be seen that the crystallinity can be increased very easily by recrystallizing the film, simply putting pure dichloromethane on them, and allowing to evaporate. The increased crystallinity had a significant effect on the behavior, as it will be shown later.

Measurements

A Teflon cell was used for the simultaneous electrochemical and microgravimetric measurements. The quartz crystal was sealed by rubber O rings, leaving one
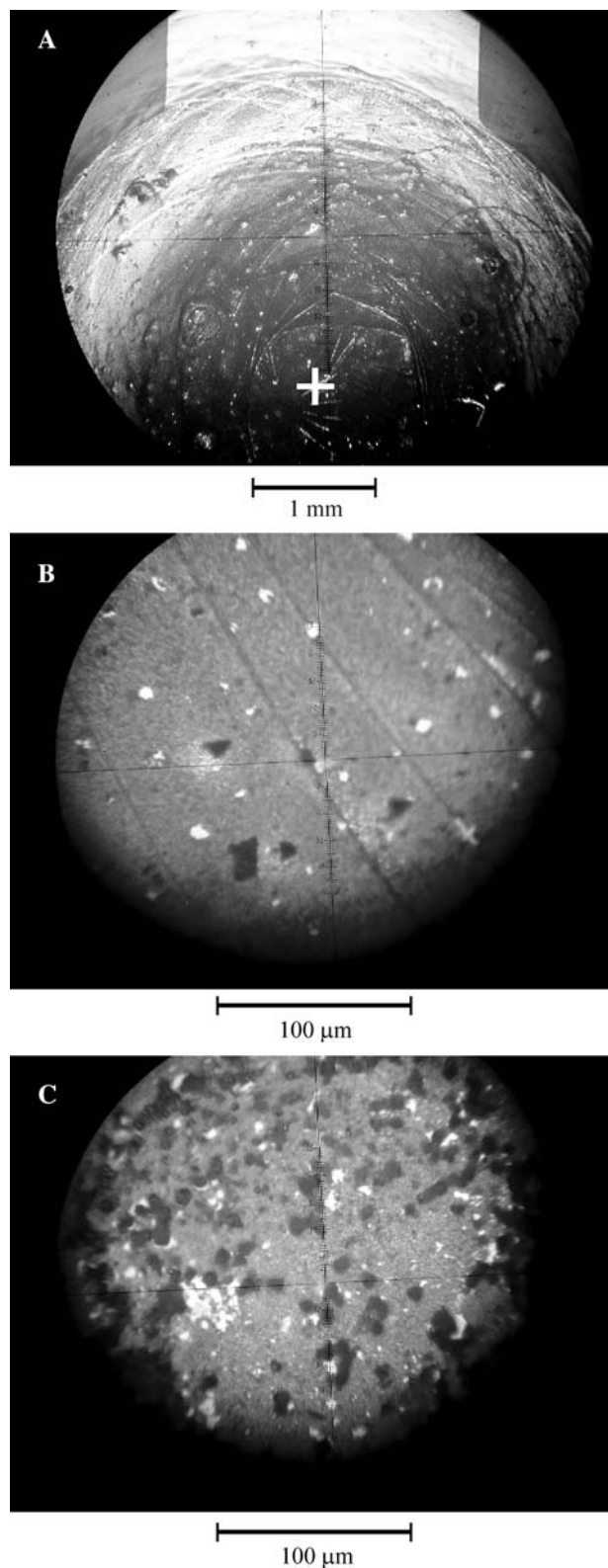

Fig. 1 Pictures of a C_{60} film on the surface of a quartz crystal. **a** Low magnification, the white cross shows the center of the electrode surface; **b** higher magnification of a part of the electrode surface; **c** the same film, but after recrystallization with dichloromethane

side for open air. On the other side, 2 cm^3 of the solution was filled into the cell, and a gold coil counter electrode was placed in it. A saturated calomel reference electrode (SCE) was connected to the cell by a Luggin capillary. (It was measured that the half potential of the reactions of ferrocene/ferrocenium couple occurred at 0.22 V versus SCE, i.e., 0.00 V versus SCE corresponds to 0.18 V versus standard hydrogen electrode [19]. However, since we used the same solution and the same electrodes in the studies, we give all the potentials versus SCE. Before each measurement, the solution was de-aerated by nitrogen gas. In order to minimize the changes in the composition of the solution, nitrogen was saturated with dimethylformamide before bubbling to the cell. During the measurements, nitrogen flow was stopped. The quartz crystal was operated by a lever oscillator (ICM 35366, 10 MHz), and the frequency was measured by a Hewlett Packard universal counter (53131A). The electrochemical measurements were done by an Electroflex potentiostat (EF 453). The electrochemical and the frequency data were collected using an IBM PC computer.

Results and discussion

A voltammogram of a C_{60} film formed from 50 μl of 300 μM solution can be seen in Fig. 2. Starting from 0.00 V, two reduction peaks developed at −0.83 and at −1.05 V, respectively. The first reduction process was accompanied with a frequency decrease followed by a smaller increase. The second reduction caused a huge frequency increase. The overall charge for the reductions was 1,470 μC, i.e., 7.62 nmol (5.49 μg) C_{60} reacted in two consecutive one-electron steps. (The expected amount of C_{60} would have been 15 nmol (10.80 μg), calculated from the volume and the concentration of the solution used for casting. Probably, the difference is due
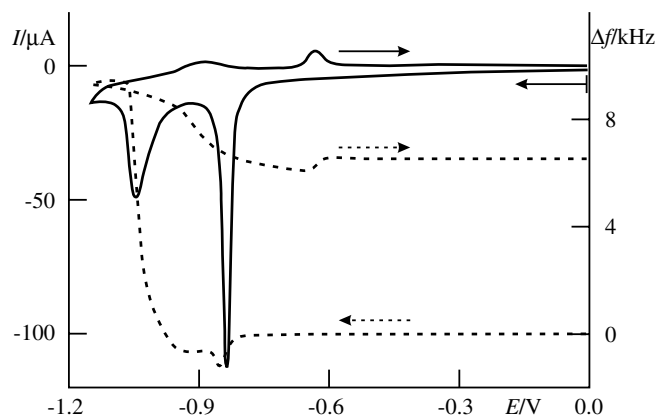

Fig. 2 Cyclic voltammetry and simultaneous microgravimetry of a C_{60} film deposited from 50 μl solution. The solution was 48 v/v% DMF + water mixture containing 1 M KCl. The potential range corresponds to the first and second reduction and reoxidation. *Solid line* current; *dashed line* frequency change during the cycle. The *arrows* indicate scan directions. The scan rate was 5 mV s^{-1}

to C_{60} that spread on the quartz plate, and not on the gold disc.) The overall change in the frequency was 9.50 kHz, which would correspond to about 8.17 μg decrease in the mass of the electrode. (The mass change was calculated by the 0.86 ng Hz^{-1} mass sensitivity of the microbalance. However, we should note, that this mass sensitivity would be strictly valid only for uniform films, which we definitely did not have, see Fig. 1. Nevertheless, we will give the mass equivalent of the measured frequency changes to indicate the order of magnitude. However, it should be mentioned that structural change alone of the film (e.g., the change in density) could result in a frequency change. So, the mass values should be considered as approximations. The calculated mass decrease suggests that the whole film of C_{60} dissolved during the second reduction. The larger mass change than the amount of electroactive C_{60} indicates that the original film contained some entrapped solvent, dichloromethane, used for casting the film. We could estimate from the ratio of C_{60} and the overall mass change, that about 2.68 μg (31.56 nmol) CH_2Cl_2 could be in the film, i.e., about 4 CH_2Cl_2 molecules were trapped with each C_{60} molecule. (The presence of entrapped CH_2Cl_2 was shown earlier by reflection absorption IR measurements [20].) The backward scan displays two oxidation processes with peaks at −0.89 and −0.63 V, respectively. The oxidation charges were clearly just fractions of the reduction charges. That could mean that just a small part of the dissolved, reduced C_{60}, was available for further reactions, and that the major part diffused away from the electrode. The first oxidation process was accompanied by a significant frequency decrease, suggesting that upon oxidation, some C_{60} precipitated back to the gold surface. This solid C_{60} could then be oxidized further with a small frequency increase. The final frequency was much larger than the initial one, indicating significant loss of the film, suggested by the small value of the oxidation charge, as well. From the frequency (mass changes), it is clear that the first reduction could be considered as a completely surface-confined process. The second reduction produced dissolved species, but those could precipitate from about −0.95 V back to the electrode. That suggests that keeping the potential above −0.95, we could study exclusively solid-state transformations of the films.

In Fig. 3, the result of a potential cycle can be seen between 0.00 V and −0.90 V for a C_{60} film cast from a 50 μl solution. The reduction peak was at −0.84 V, and the corresponding oxidation peak was at −0.64 V. In this experiment, the charges of the reactions of C_{60} were 880 μC for the reduction, and 860 μC for the oxidation, i.e., little larger than those in the earlier example, shown in Fig. 2, but the peak positions were very similar. The reduction caused a large frequency decrease, $\Delta f = -6.87$ kHz (measured at −0.75 V potential between the forward and reverse scans), indicating a significant increase in the mass of the film, m = 5.91 μg. Considering the amount of C_{60}, calculated from the reduction charge (9.12 nmol), the molar mass change would cor-
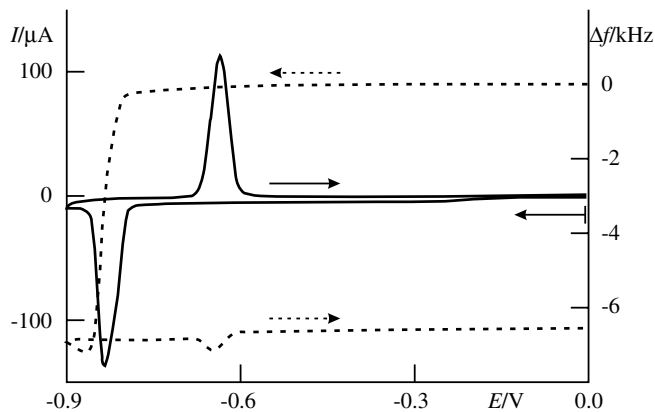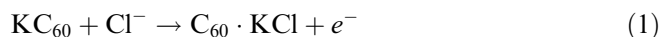
Fig. 3 Cyclic voltammetry and simultaneous microgravimetry of a C_{60} film deposited from 50 µl solution. The potential range was restricted to the first electrochemical reaction. *Solid line* current; *dashed line* frequency change during the cycle. The *arrows* indicate scan directions. The scan rate was 5 mV s^{-1}

Fig. 4 Cyclic voltammetry and simultaneous microgravimetry of a C_{60} film deposited from 50 µl solution. *Solid line* current; *dashed line* frequency change during the cycle. **a** First cycle; **b** second cycle. The scan rates were 20 mV s^{-1}. The frequency change ($\sum \Delta f$) was measured from the initial frequency before starting the first scan

respond to 648 g mol^{-1}. This is obviously much larger than the 39.1 g mol^{-1} expected for merely K$^+$ ion uptake to compensate the negative charge on C_{60} molecules, i.e., to form KC$_{60}$. Moreover, it was shown earlier, that a significant amount of entrapped CH_2Cl_2 could be removed from the film by a single cycle [20], which would have caused a frequency increase. That is, we have to assume that the uptake of K$^+$ occurred with a very significant swelling of the film, the ionic compound became partially solvated, and that resulted in a huge frequency decrease. (We should note that the microgravimetry data are cumulative results of the swelling, i.e., the change in the structure of the film, and the real mass change, so the quantitative interpretations are just approximations.) On the reverse scan, at the beginning of the oxidation process, there is a $\Delta f = -0.34$ kHz further decrease in the frequency, which is followed by a $\Delta f = 0.63$ kHz increase. Thus, the overall frequency change upon oxidation was merely 0.29 kHz. That would suggest that upon oxidation the solvent remained entrapped in the film. The frequency decrease at the beginning of the oxidation process could mean the uptake of Cl$^-$ ions to form some inclusion complex of C_{60} and KCl,

$$KC_{60} + Cl^- \rightarrow C_{60} \cdot KCl + e^- \tag{1}$$

and the following frequency increase could mean the release of K$^+$ ions,

$$KC_{60} \rightarrow C_{60} + K^+ + e^- \tag{2}$$

When we repeated the experiment discussed above, to see the effects of experimental conditions (such as film thickness, sweep rate, or applying potential step instead of sweeps) we were surprised, how much the quantitative results were changed. Figure 4a shows, for example, the experimental findings on a similar layer as was shown in Fig. 3, but with a scan rate of 20 mV s^{-1} instead of 5 mV s^{-1}. The shape of the voltammogram did not
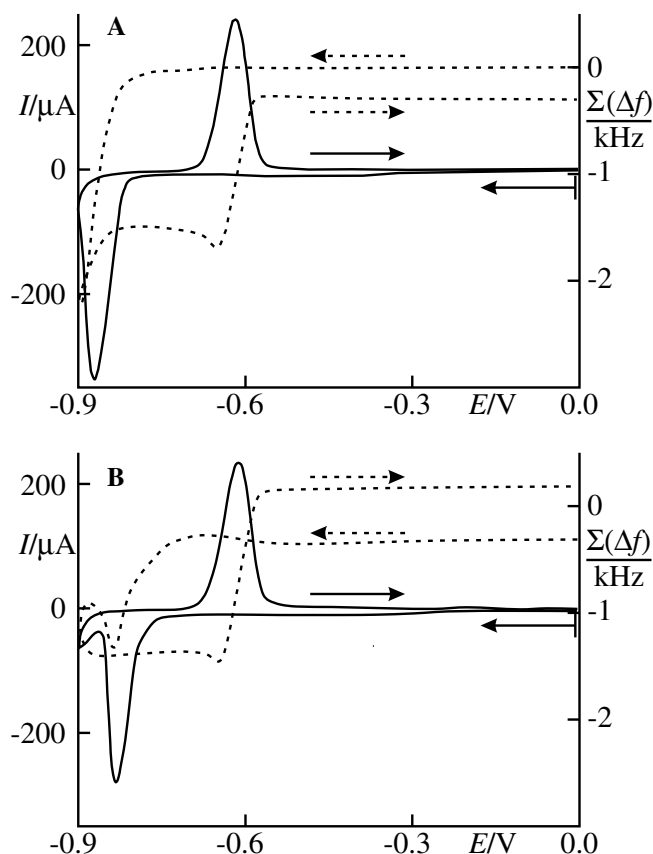
change too much, however, the frequency change altered very significantly. The charges for the reduction and oxidation of C_{60} were 780 and 740 µC, respectively. The overall frequency change upon reduction was just $\Delta f = -1.49$ kHz. That is, the amount of electroactive C_{60} was 8.08 nmol, and the resultant mass increase was 1.28 µg. By those, the molar mass increase would be only 158 g mol^{-1}, much smaller than for Fig. 3, which might suggest significantly less swelling. Furthermore, the frequency change upon oxidation, $\Delta f = 1.42$ kHz was much larger than previously, and the film had almost the same mass as at the beginning of the experiment. As if now almost all the solvent went out of the film. Only the frequency decrease at the beginning of the oxidation was similar to the previous one, it was about $\Delta f = -0.22$ kHz. Figure 4b shows the second scan on the same film. The reduction and oxidation charges were 740 µC, similar as in the first scan, but the reduction peak potential shifted to positive direction by about 40 mV. The reduction became easier by the first scan. It can also be seen that the frequency increased after the second scan even above the initial value, the film became lighter than it was originally. It was very surprising that on the reduction half cycle, the frequency "oscillated". It increased slightly
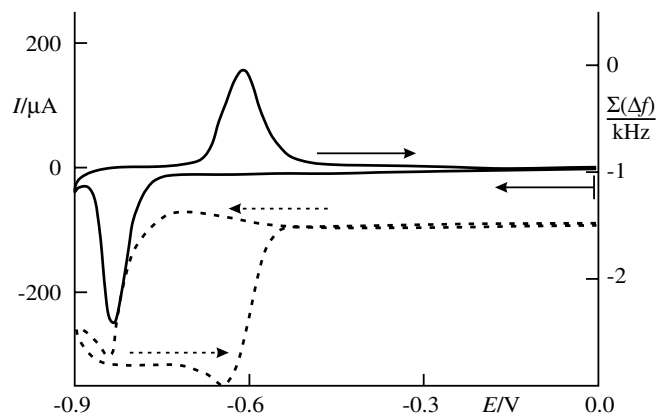
Fig. 5 Simultaneous cyclic voltammetry and piezoelectric microgravimetry curves for the C_{60} film of Fig. 4. The eighth scan is shown. *Solid line* current; *dashed line* frequency change during the cycle. The scan rate was 20 mV s^{-1}. The frequency change ($\sum \Delta f$) was measured from the initial frequency before starting the first scan

from about −0.53 V, decreased from −0.68 V, increased again from 0.83 V, and decreased again from −0.88 V. We observed such behavior for any further scans (see Fig. 5 for the eighth scan). The only difference was that the starting and ending frequency approached each other by the continuous scans, and after four to five scans we reached some kind of "steady-state" behavior. Later, we realized that the change in behavior discussed above was not the consequence of the change in the scan rate. Whenever we repeated the experiments, we just could not predict the results; they seemed to be absolutely random. Neither the scan rate, nor the amount of C_{60} put on the surface seemed to have a clear effect. An illustration of that can be seen in Fig. 6, for some collected experiments. All those were measured with 20 mV s^{-1} scan rate, but the volume of the solution sample dispensed onto the electrodes varied from 15 µl to 50 µl. In Fig. 6a, it can be seen that the overall change in frequency ($\sum \Delta f$), measured from the initial frequency of the first scan could vary in a very wide range, and apparently it does not show correlation with the amount of C_{60}. For instance, using a 50 µl solution sample, the overall frequency decrease could be either smaller or larger than those for films formed from 25 or 15 µl solutions. Even more, in some cases (with a recrystallized film, see Fig. 1c), the overall change could be a frequency increase (see Fig. 6a fourth measurement). In Fig. 6b, the separated scan by scan cathodic and anodic changes can be seen for some of the measurements (here the frequency change was measured from the initial frequency of each scan). The beginning is quite random again, but after the fifth cycle we can see some proportionality to the amount of C_{60} put on the surface. This proportionality is clearer from Fig. 6c, where the scan by scan frequency changes over the corresponding reduction or oxidation charges were plotted. From the fifth scan, we obtained a constant change, about −2 Hz µC^{-1} for the reduction and 2 Hz µC^{-1} for the oxidation, independently of the
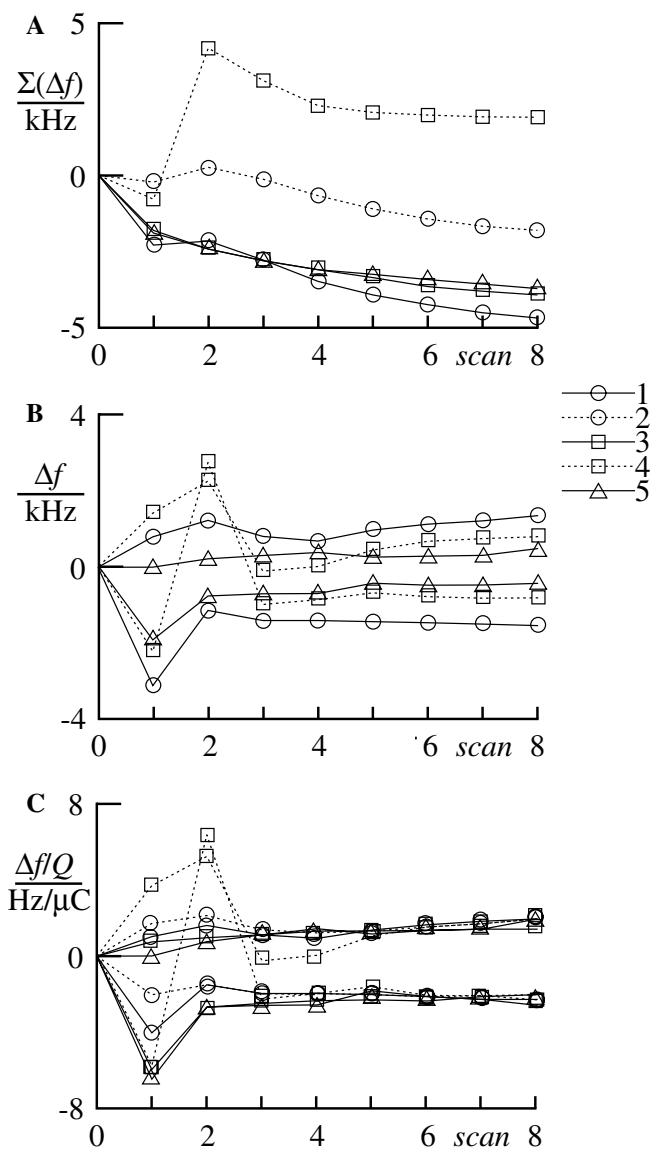

Fig. 6 Frequency changes with various fullerene films on the electrodes as the function of the scan number. **a** The overall frequency changes for five different films; **b** the scan by scan cathodic and anodic changes for three of the films; **c** the scan by scan frequency changes referred to unit charge. *1* 50 µl C_{60} (750 µC); *2* 50 µl C_{60} (720 µC); *3* 25 µl C_{60} (380 µC); *4* 25 µl C_{60}, and recrystallized (370 µC); *5* 15 µl C_{60} (290 µC). The scan rates were 20 mV s^{-1} in each case

amount of C_{60}. This amounts correspond to about 166 g mol^{-1} molar mass changes, as a "steady-state" value (see Fig. 5, too). So, we can conclude that the initial changes are quite unpredictable, however, all the films approach a "steady-state" behavior after a few scans. We may discuss this steady-state behavior in detail first, and then, we may try to find the reason for the random behavior at the beginning of the measurements.

There are five distinct features on the steady-state microgravimetric curves (see Fig. 5 again). We may plot the frequency changes as the function of time and as the function of charge (background corrected), too (see
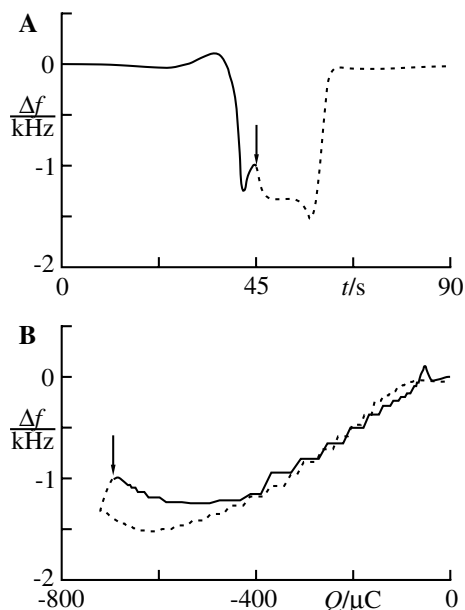
Fig. 7 Conversions of the "steady-state" frequency changes (shown in Fig. 5) as the function of: **a** time; **b** charge. The *arrow* indicates the scan reversal. *Solid line* cathodic scan; *dashed line* anodic scan

Fig. 8 Voltammetry and simultaneous microgravimetry of a C_{60} film deposited from 25 µl solution and after reaching the steady-state (after eight cycles between 0 and −0.9 V). **a** current (*solid line*) and frequency change (*dashed line*) between 0 V and −0.7 V. The scan rate was 20 mV s^{-1}. **b** The overall frequency change as the function of scan number

Figs. 7a, b) in order to separate the time and charge dependency. It seems that the first frequency increase is not connected to real Faradaic processes. The following frequency decrease and increase have charge dependence. After reversing the scan direction the additional frequency decrease seems rather time- than charge dependent. On the reverse scan, both the frequency decrease and the following frequency increase have similar charge dependency as on the forward scan. The first small frequency increase (mass decrease) before the reduction peak occurs from about −0.53 V. When we restricted the potential scan to this region (Fig. 8a), we could see no apparent Faradaic process, only a strange-looking, broadening capacitive current curve. The current was proportional to the scan rate at any potential, and hardly changed with repetitive scans. However, the frequency increased scan by scan as shown in Fig. 8b. One consequence of such scans was that the system got out of the steady-state. When we extended the potential range again till −0.90 V, the reduction peak shifted by 20 mV to negative direction, and the frequency change became larger (in absolute value) upon reduction. The second scan in this wider potential range displayed the steady-state behavior again. Earlier, it was shown that before the bulk reduction of a C_{60} film, we have to assume a partial reduction involving only the surface of the film [21]. In this potential region, we could produce hydrogenized C_{60} in acidic solution [20], so we may suggest the formation of HC_{60} to some extent by the reaction
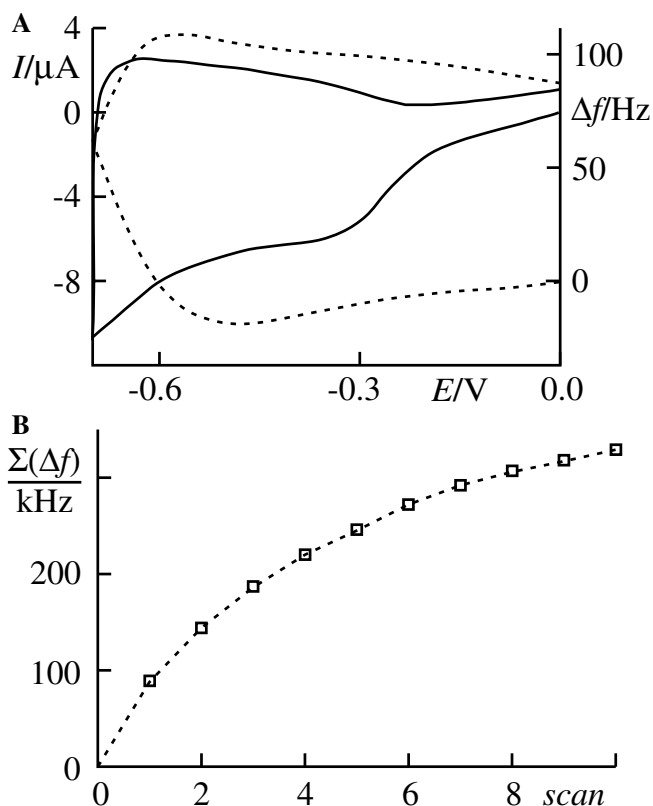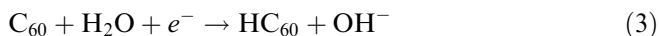
$$C_{60} + H_2O + e^- \rightarrow HC_{60} + OH^- \tag{3}$$

However, HC_{60} is a weak acid, so it can dissociate, or in other words it can produce a potassium salt by ion exchange

$$HC_{60} + K^+ \rightarrow KC_{60} + H^+ \tag{4}$$

Since above −0.70 V, we are in the region of the oxidation of KC_{60},

$$KC_{60} \rightarrow C_{60} + K^+ + e^- \tag{5}$$

we may say that the reduction of C_{60} is short-circuited by the ion-exchange equilibrium, resulting in a current which looks like a mere capacitive current. However, the

$$C_{60} \rightarrow HC_{60} \rightarrow KC_{60} \rightarrow C_{60} \tag{6}$$
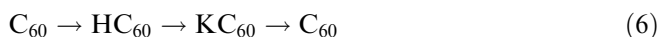
cycle rearranges the films. The solvent (or ions), entrapped in earlier cycles, could move out from the hydrophobic environment, resulting in a mass decrease. The film slowly approaches the initial state, and that can be seen in the shift of the reduction peak potential, too.

The second change accompanies the beginning of the bulk reduction of the films, and it is a large frequency decrease (mass increase). It can simply be assumed as the consequence of partially solvated K^+ uptake into the film

$$C_{60} + K^+(\text{solv}) + e^- \rightarrow KC_{60}(\text{solv}) \qquad (7)$$

From the initial slope of the frequency change versus reduction charge (Fig. 7b), we can estimate about 260 g mol^{-1} molar mass change, emphasizing the solvation. The following frequency increase was a little bit puzzling. It was never observed on the first scans (see, e.g., Fig. 4a), i.e., this feature was missing from a freshly prepared film. We suggest that this is the consequence of Eq. 1, i.e., the presence of Cl^- ions entrapped in previous scans. That is the reduction could proceed as

$$C_{60} \cdot KCl + e^- \rightarrow KC_{60} + Cl^- \qquad (8)$$
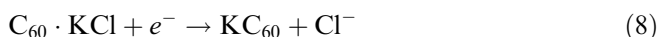
as well. After reversing the scan direction some further swelling of the ionic film might be suggested. During the oxidation, processes that are opposite to that of Eqs. 8 and 7 occur, taking the film back into the initial stage, that is forming some partially solvated $C_{60} \cdot KCl$.

It is interesting that although the reduction and oxidation are single peaks on the voltammograms (in any stage), microgravimetry clearly shows that those are complex processes. Both involve uptake and release of (probably solvated) ions, and it seems that the ion uptake always proceeds the ion release. However, their energy requirements are about the same. This can be seen better, if instead of a potential scan, we reduce the film (already reached the steady-state) by a potential step. Figure 9a shows the result of a simultaneous microgravimetry and double potential step chronoamperometry experiment. The initial potential was -0.45 V and the potential was stepped to -0.90. When the frequency reached a constant value, the potential was jumped to -0.45 V again. It can be seen that the time and the charge dependence of the frequency were very similar to a potential scan experiment (see Fig. 7), except for the large charging due to the potential jump. (The time resolution of the frequency measurement was low, that is why the frequency curve shows steps.) Here, it can be seen again that the bulk reduction of the fullerene film composed of a K^+ uptake and a Cl^- release, was followed by some swelling. The opposite potential jump indicates only the K^+ release, but since the resolution of frequency measurement was low, we cannot exclude Cl^- inclusion, as well. From the figure, it can also be seen that although the film was in steady-state before the potential step experiment, it got out of it, since the frequency changed by about -1 kHz at the end of the double potential step experiment. The film became heavier, probably more solvated than before. We observed, however, that after a few potential cycles, it went back to the original "steady-state". It seems that the complexity of the reduction-oxidation processes (the desolvation during the partial reduction, the uptake of solvated K^+ ions, the release of Cl^- ions, the further solvation of the ionic compound of C_{60}, the uptake of Cl^- ions, the release of K^+ ions in one potential cycle) makes the system very sensitive. Any change (sweep rate, potential jump instead of a scan) can perturb the events, their magnitudes. However, it is very important to emphasize that the system self-adjusts, it can reach a
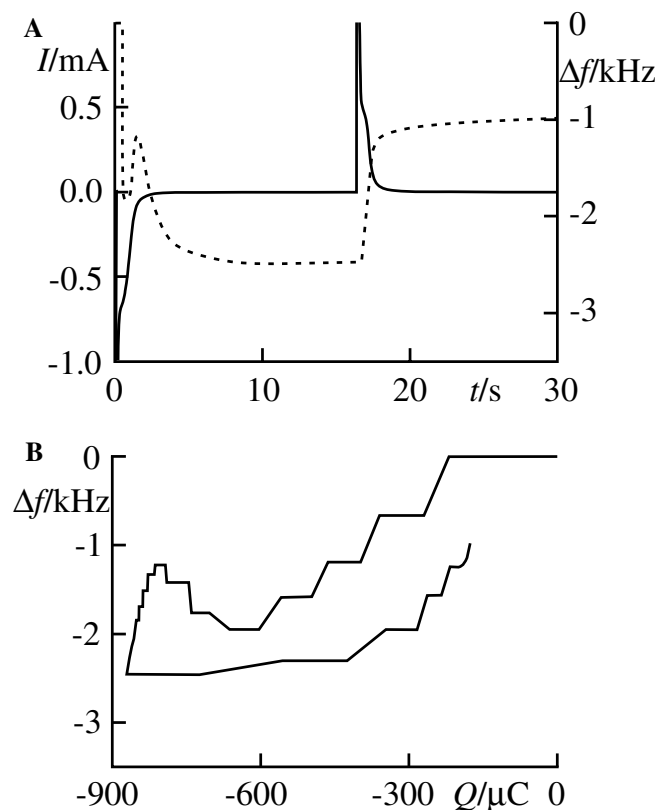

Fig. 9 Double potential step chronoamperometry experiment on a fullerene film deposited from 50 μl solution, and after the steady-state behavior was reached. **a** Current and frequency changes versus time; **b** the frequency change versus charge. The initial potential was -0.45 V. The potential was stepped to -0.90 V and then back to -0.45 V
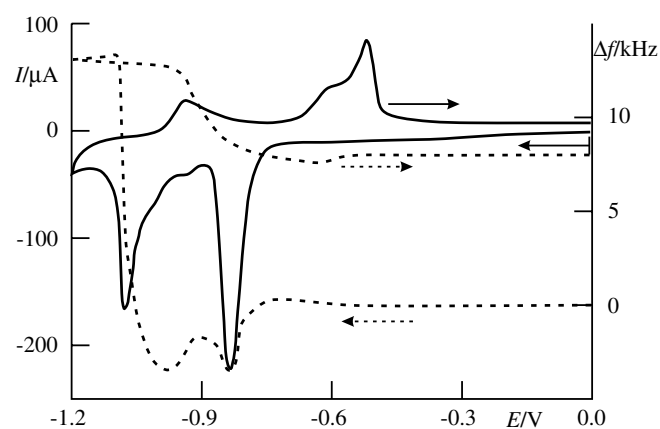

Fig. 10 Cyclic voltammetry and simultaneous microgravimetry of a C_{60} film deposited from 50 μl solution, and after reaching the steady-state (after eight cycles between 0 V and -0.9 V). The potential range corresponds to the first and second reduction and reoxidation. *Solid line* current; *dashed line* frequency change during the cycle. The *arrows* indicate scan directions. The scan rate was 20 mV s^{-1}

steady-state, and it can return to this steady-state after any perturbation.

Finally, we should show the extended voltammogram of a film which reached the steady state. Figure 10 indicates that the basic features are the same as with freshly prepared films (see Fig. 2). The film became soluble and was removed from the surface when the second reduction began. The corresponding frequency change, which is usually larger than with freshly prepared films, suggests that the whole, partially solvated film dissolved, and just a fragment of C_{60}^{2-} could be precipitated back to the electrode surface

After analyzing the steady-state behavior, it is now easy to explain the "random" behavior of various measurements (see Fig. 6). The initial behavior depends on the initial structure of the film, how far it is from the steady-state structure. The steady-state behavior assumes a rather porous structure, providing channels for the ion movement in and out. If the initial structure lacks these channels, more significant rearrangement is needed to reach the steady-state. Also, we have to consider the presence of dichloromethane in the initial film, which could escape upon cycling, thus contributing to the mass change (frequency change) in the first few potential cycles. Our technique to make the films was rather simple, and considering just the voltammetric responses, it was reproducible, too. However, we have no way of controlling the crystallinity, the porosity of the film, and also the amount of entrapped solvent, CH_2Cl_2 used for solution casting could vary with each experiment. That means that the overall frequency changes during the first scans were the results of several changes in the structure of the films, and since the initial structure was "random", the resulting change was random, too. This can be emphasized by the example, when we made a definitely more crystalline film on purpose (see Fig. 1c, and Fig. 6a fourth measurement). Its initial behavior is far out of average, probably due to a larger amount of entrapped dichloromethane, as well, however, its "steady-state" behavior just perfectly fits the others. Even this "bad" film was self-adjusted to the conditions.

Conclusions

Quartz crystal microbalance studies on solution cast C_{60} films showed that the solid-state reactions of this fullerene are rather complex. It involves the movement of solvent, cations and anions, as well. The measurements emphasized the effect of the initial structure of the fullerene films on the behavior, but also indicated the self-adjustment of the films to the conditions. It is an interesting question how much this behavior is characteristic to the present experimental conditions, how much it can change with the solution composition, or with the change of counter cations. Further studies are under way to answer these questions.

References

1. Jehoulet C, Bard AJ, Wudl F (1991) J Am Chem Soc 113:5456
2. Koh W, Dubois D, Kutner W, Jones MT, Kadish KM (1992) J Phys Chem 96:4163
3. Compton RG, Spackman RA, Wellington RG, Green MLH, Turner J (1992) J Electroanal Chem 327:337
4. Zhou F, Yau SL, Jehoulet C, Laude DA, Guan Z, Bard AJ (1992) J Phys Chem 96:4160
5. Jehoulet C, Obeng YS, Kim YT, Zhou F, Bard AJ (1992) J Am Chem Soc 114:4237
6. Compton RG, Spackman RA, Riley DJ, Wellington RG, Eklund JC, Fisher AC, Green MLH, Doothwaite RE, Stephens AHH, Turner J (1993) J Electroanal Chem 344:235
7. Koh WY, Dubois D, Kutner W, Jones MT, Kadish KM (1993) J Phys Chem 97:6871
8. Tatsuma T, Kikuyama S, Oyama N (1993) J Phys Chem 97:12067
9. Chlistunoff J, Cliffel D, Bard AJ (1995) Thin Solid Films 257:166
10. Wang WJ, Chiu HS, Yu LJ, Wang BC (1995) Synthetic Met 70:1439
11. Wang WJ, Chiu HS, Lin SS, Chang CS, Chuang KS (1998) Fullerene Sci Techn 6:681
12. Suarez MF, Marken F, Compton RG, Bond AM, Miao WJ, Raston CL (1999) J Phys Chem B 103:5637
13. Bond AM, Miao WJ, Raston CL (2000) J Phys Chem B 104:2320
14. Bond AM, Feldberg SW, Miao WJ, Oldham KB, Raston CL (2001) J Electroanal Chem 501:22
15. Tan WT, Lim EB, Bond AM (2003) J Solid State Electr 7:134
16. Balch AC, Costa DA, Fawcett WR, Winkler K (1997) J Electroanal Chem 427:137
17. Szucs A, Budavari V, Nagy JB, Novak M (2002) J Electroanal Chem 528:153
18. Sauerbrey G (1959) Z Phys 155:206
19. Milazzo G, Caroli S, Sharma VK (1978) Tables of standard electrode potentials. Wiley, New York
20. Szucs A, Budavari V, Berkesi O, Novak M (2003) J Electroanal Chem 548:131
21. Szucs A, Tolgyesi M, Csiszar M, Nagy JB, Novak M (1998) Electrochim Acta 44:613